TP-18 189

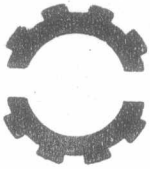

MILITARY TECHNICAL COLLEGE
CAIRO - EGYPT

FORCES PREDICTION DURING CUTTING WITH CONTROLLED CONTACT LENGTH TOOLS

M. Abd El - MONEIM * , M.M. ELKHABEERY **

ABSTRACT

Forces induced upon the dry orthogonal cutting of 2024 Aluminum alloy employing controlled contact length tools are predicted via two published models developed by Abdel Moneim.
The experimental data, at a cutting speed of 120 m/min, are checked against the theoretical models.
Theoretical values for both cutting and thrust forces relevant to tool nose edge are assessed utilizing Abdel Moneim finish machining model.
The second theoretical model, offers an approximate upper bound solution for predicting the forces which act upon inclined straight tool rake surfaces utilizing a simplified slip-line field technique.
Such two models, combined together, predicted the values of both cutting and thrust forces induced during machining with controlled contact length tools.
Experimental force data are recorded by the second author for orthogonal dry machining of solution treated and aged 2024 aluminum alloy at a relatively high speed (120 m/min) selected to avoid complications of active build-up formation.
Such data are found to be in fair agreements with theoretical models.

INTRODUCTION

The mechanics of finish machining has long remained a mystry due to the experinental difficulties involved in making precise physical measurements on such a small scale. In an attempt to overcome these problems, at least in part, a study of the mechanics of cutting using simulated model experiments would seem to offer some advantage [1] . In this way the uncertainties associated with the accurate measurement and maintenance of very small radii may be avoided. Agreement between observed cutting force data and the results of the theory presented in that paper [1] was obtained and this indicates that the latter may have some value in the understanding of the process, for $t \leq r\,(1 + \sin\alpha)$. Abdel Moneim [2] presented his model for finish machining for cutting within tool nose height.
However, the concept of finish machining may be extended to cover cutting

* Assistant professor, Production Engineering Department, Faculty of Engineering & Technology, Suez Canal University, Port Said, Egypt.
** Assistant Professor, Production Engineering & Machine Design Department, Faculty of Engineering & Technology, Menoufia University, Shebin El-Kom, Egypt.

small depths of cut. At such tiny depths, sticking friction condition is likely to prevail.
It is one of the objectives of the current paper is to ensure such condition. That was done by selecting controlled tool-chip contact lengths smaller than the extent of the sticking region for natural contact length tools [3].

ANALYSIS

Cutting and thrust forces induced during orthogonal cutting employing controlled contact length tools can be atributed to two main zones :
(I) Tool edge nose zone, (the first zone) and
(II) Straight tool rake face controlled contact length zone,(the second zone).
The plastic flow which occurs in each of these zones contributes to the total value of the recorded forces. Material flow within the two zones is assumed to be in a state of maximum shear and compressive stresses. No account will be made to the formation of active build-up edges during cutting.

(I) Forces Prediction for Cutting within the First Zone

The model presented here, for the tool edge nose zone is recorded [1].
Material flow within such zone is divided into two main parts, viz;
(i) A rubbing region whereby no cutting is assumed to take place. That region is located at end beneath a postion of the curved tool base (for a perfectly sharp cutting tool)
Bearing in mind the concept of circular cylinderical surfaces of velocity discontinuity adapted by Johnson [4], an upper-bound solution is developed by Abdel Moneim [1] for the plastic flow of material beneath the rubbing region.
In investigations reported in earlier papers [5 and 6], critical rake angles ranging between -75 and -80 degrees resulted in chip evolvements. Since the value suggested by Komanduri [6], viz.; -76 degrees, falls within this range, the theoretical derivation outlined in this paper employ the latter value.
The best upper-bound solution for the rubbing region is proved [1] to be as that indicated in Fig. 1.
The power rubbing force (in the direction of tool motion), F_{er}, associated with shearing at the tool base within the rubbing region ABC per unit workpiece width, is given by Eq. (1)

$$F_{er1} = \tau . \text{ ABC} . V_{2c} = 2 \tau r \theta_o / \cos \theta_o \qquad (1)$$

The power rubbing force per unit width associated with the velocity discontinuity AEC, F_{er2} is given by Eq. (2) :

$$F_{er2} = \tau . \text{ AEC} . V_1 = \pi r \sin \theta_o \tan \theta_o \qquad (2)$$

Therefore, the total rubbing force per unit width for the entire rubbing region is as given by Eq. (3) upon adding Eq. (1) + Eq. (2) (note that $\theta_o = 14\pi / 180$).

$$F_{er} = F_{er1} + F_{er2} = \tau r \left(\frac{2 \theta_o}{\cos \theta_o} + \pi \sin \theta_o \tan \theta_o \right) \qquad (3)$$

The thrust force per unit workpiece width, F_{tr}, normal to the cutting

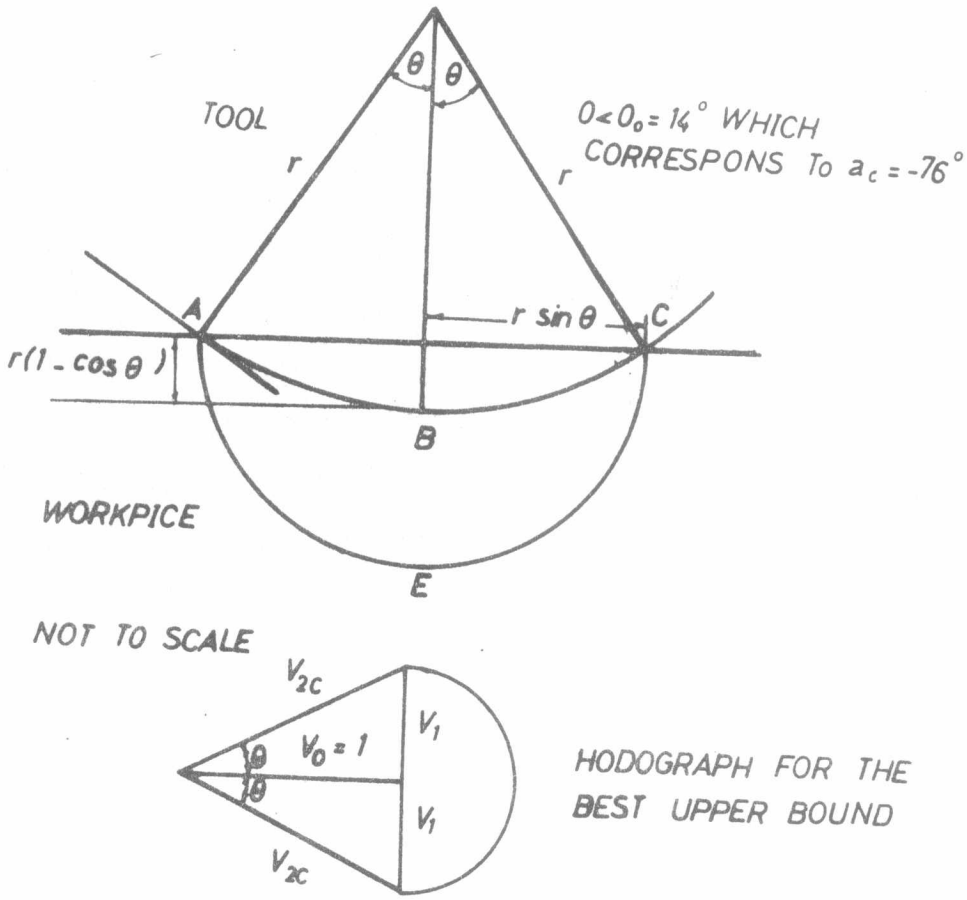

*Fig.1. **Best upper bound solution for the rubbing region***

velocity vector, due to material bearing on the boundary ABC (for a von Mises material in which the normal stress is equal to $\sqrt{3}$), is given by Eq. (4) :

$$F_{tr} = 2\sqrt{3}\,\tau\, r \sin\theta_o \qquad (\theta_o = 14\pi/180) \tag{4}$$

(ii). The cutting region in which a stable build-up formation is assumed to cover the rest of the tool edge nose zone above the rubbing region. The power cutting force within the cutting region consists of two parts, as indicated in Fig. 2, viz ;

(a) That part which is due to the chip sliding over the stable built-up, F_{ecl} , and

(b) That part which has its origin in the rubbing of the workpiece over the lower surface of the stable built-up. Referring to Fig. 2, it may be seen that,

$$F_{ecl} = P(\cos\alpha_f)\left\{t - r(1-\cos\theta_o)\right\}/\cos\alpha_f + \tau(\sin\alpha_f)\left\{t - r(1-\cos\theta_o)\right\}/\cos\alpha_f = \tau r\left\{\frac{t}{r} - (1-\cos\theta_o)\right\}\left(\frac{P}{\tau} + \tan\alpha_f\right) \tag{5}$$

where P is the pressure exerted by the workpiece material over the tool edge (as estimated approximately in the Appendix), t is the undeformed chip thickness, and

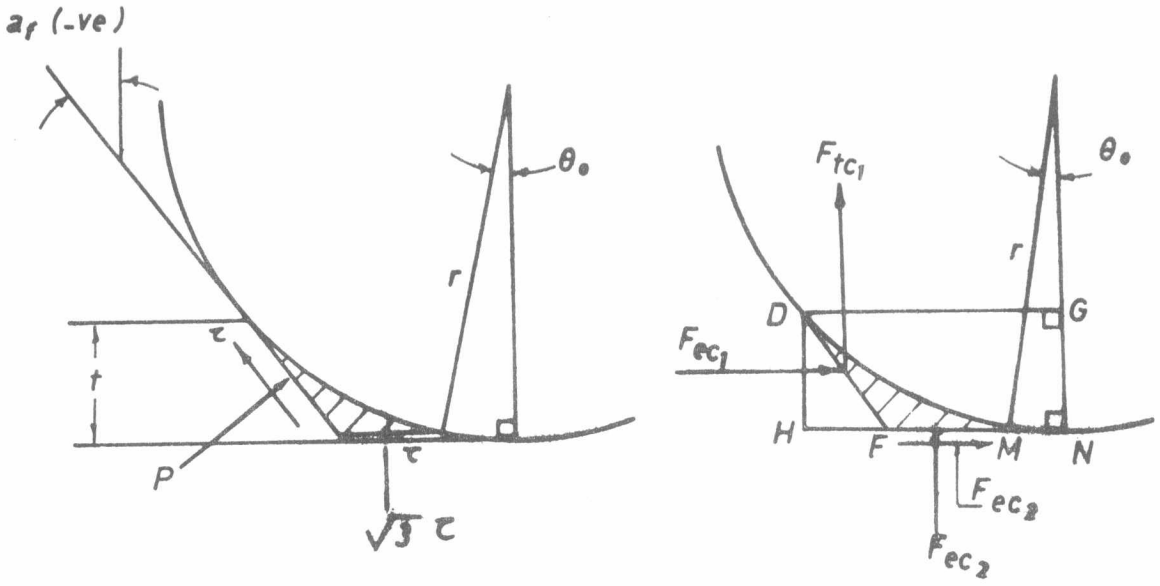

Fig. 2. Force balance for the cutting region

$$\alpha_f = -\sin^{-1}\left(1 - \frac{t}{r}\right) \tag{6}$$

It also follows from the force balance that

$$F_{ec2} = \tau \cdot FM$$

$$= \tau r \left\{(\tan\alpha_f)\left(\frac{t}{r} - 1 + \cos\theta_o\right)\cos\alpha_f - \sin\theta_o\right\} \tag{7}$$

The total power cutting force per unit workpiece width, F_{ec}, is the sum of F_{ec1} and F_{ec2}

Similarly, it can be proved that

$$F_{tc1} = \tau r \left\{\left(\frac{t}{r} - 1 + \cos\theta_o\right) - \left(\frac{P}{\tau}\right)\tan\alpha_f\right\} \tag{8}$$

$$\& \quad F_{tc2} = \sqrt{3}\,\tau r \left\{(\tan\alpha_f)\left(\frac{t}{r} - 1 + \cos\theta_o\right) + \cos\alpha_f - \sin\theta_o\right\} \tag{9}$$

The total thrust force per unit workpiece width, F_{tc}, is the sum of F_{tc1} and F_{tc2}

Therefore, total power cutting force components, F_{ec} per unit workpiece width for the first zone-that of tool nose edge height, can be predicted approximately by adding Equations (3),(5), and (7). Whereas F_{et} can be obtained by adding Equations (4), (8), and (9). It should be noted that (θ) is to be taken as $14\pi/180$ while (α_f) is equal to $10\pi/180$.

(II) Forces Prediction for Cutting within the Second Zone

The forces acting upon the straight portion of the controlled contact length tool can be predicted via the model obtained in the Appendix.

Equation (A.3) yields an approximate value of the unit pressure (P) acting upon the restricted controlled rake straight surface of $(2.221)\tau$ for $\alpha_f = 10\pi/180$ radians as used in the experimental part .

Referring to Fig. A-1, it can be proved that the power cutting force per

unit workpiece for the second zone, F_{se}, is equal to :

$$F_{se} = P\, \ell_s \cos\alpha_f - \tau \sin\alpha_f\, \ell_s = 2.036\, \tau \ell_s \quad (\text{for } \alpha_f = 10\pi/180) \qquad (10)$$

while the thrust force per unit workpiece width for the second zone, F_{st}, equals to :

$$F_{st} = P\, \ell_s \sin\alpha_f + \tau \cos\alpha_f\, \ell_s = 1.373\, \tau\, \ell_s \quad (\text{for } \alpha_f = 10\pi/180) \qquad (11)$$

Therefore, by adding theoretical force values for both zones, the total power cutting per unit workpiece width, F_e, is proved to be equal to ;

$$F_e = \tau_r \left\{ \left(\frac{28\pi}{180 \cos 14} + \pi \sin 14 \tan 14 \right) + (\sin 10 + \cos 14)(2.221 + \tan 10) + \tan 10 (\sin 10 + \cos 14) + \cos 10 - \sin 14 + \frac{2.036\, \ell_s}{r} \right\} \qquad (12)$$

From (12), hence, $F_e = \tau_r \left(4.48 + \frac{2.036}{r}\, \ell_s\right)$

Likewise, the total thrust force per unit workpiece width, F_t, is equal to;

$$F_t = \tau_r \left\{ 2\sqrt{3} \sin 14 + (\sin 10 + \cos 14) - 2.221 \tan 10 + \sqrt{3} \tan 10 (\sin 10 + \cos 14) + \cos 10 - \sin 14 + \frac{1.373\, \ell_s}{r} \right\} \qquad (13)$$

From (13) , hence, $F_t = \tau_r \left(2.97 + \frac{1.373}{r}\, \ell_s\right)$

EXPERIMENTAL WORK

The employed machine was a 5 horse power, Cincinnati Hydroshift lathe Model LR. It is equipped with a tachometer generator and has continuously variable spindle speeds in the range from 8 to 1500 rpm. The lathe has a feed range from 0.015 to 1.52 mm/rev [3] .

In addition, a three-component cutting force dynamometer was used for measuring the cutting and thrust components of the resultant force. A type SE 6150 UV oscillgraph (Kisteler Instruments AG) incorporated with a 6-channel conditioning amplifier was used. Three type 5001 change amplifiers (Kisteler) were used for transforming electro-static charges into proportional voltages. They have direct calibration factor adjustment. Also, three type 5111 A galvanometer amplifiers (Kisteler) were used for driving the UV recorder. They offer electronic overload protection of the recorder. The dynamometer has a piezo-electric 3-component measuring plateform, with high resolution, high rigidity, and minimum deflection, It is capable of measuring dynamic and quasistatic loads (forces) in three mutually perpendicular directions up to 5 KV, with high sensitivity and maximum linearity error of $\pm$ 1 percent. The dynamometer was calibrated before each set of tests[3].

Workpieces of 2024-Aluminum alloy of the following weight percentage. Copper : 3.8 - 4.9. Mangenese : 0.3 - 0.9, Magnesium : 1.2 - 1.8, Silicon : 0.5 , Iron : 0.5, Chromium : 0.1, Zinc : 0.25, Titainum : 0.15 and with the balance Aluminum; were employed. Such alloy is probably the best known and most widely used in aircraft industry. It was decided to use ring-shaped workpieces. After preparation, the test pieces were solution treated and artificially aged by heating to 493 C, soaking for 1 hour, quenching in cold - 8 % aqueous solution of Sodium Chloride, reheating to 191 C for 8 hours to be followed by air cooling to room temperature. Convential tensile tests for such specimens yielded a value of the ultimate strength to be

517 MN/m^2 and yield strength equals to 490 MN/m^2 [3] .
High speed steel tools (T - 15) of 12.75 mm square section and of 65 Rc hardness were utilized. Controlled tool-chip contact lengths of 0.25, 0.50, and 0.75 mm with a primary rake face angle of 10 degrees were ground. Sticking were found to cover the entire primary rake faces for all of the employed tools [3] .
Orthogonal tests conditions were as follow ; cutting speeds = 6, 12, 24, 48, 96, 120, and 186 m/min, feed (depth of cut) : 0.128 mm. Tests under dry and lubricated conditions were performed.

RESULTS AND DISCUSSION

The cutting speed was found to influence both of cutting and thrust force components for speeds less than 48 m/min. This is understandable, particularly in presence of active build-up formation. However, at higher speeds, constant values of both cutting and thrust force components, dependant only on the chip-tool contact length (ℓ_s), were obtained. Figure (3) shows the linear relationships between both of the force components per unit workpiece width, F_c, and tool-chip contact length (ℓ_s) for dry orthogonal conditions. Vertical axis intercepts represent zero tool-chip contact length and the situation upon cutting with a depth of cut equals to the nose edge

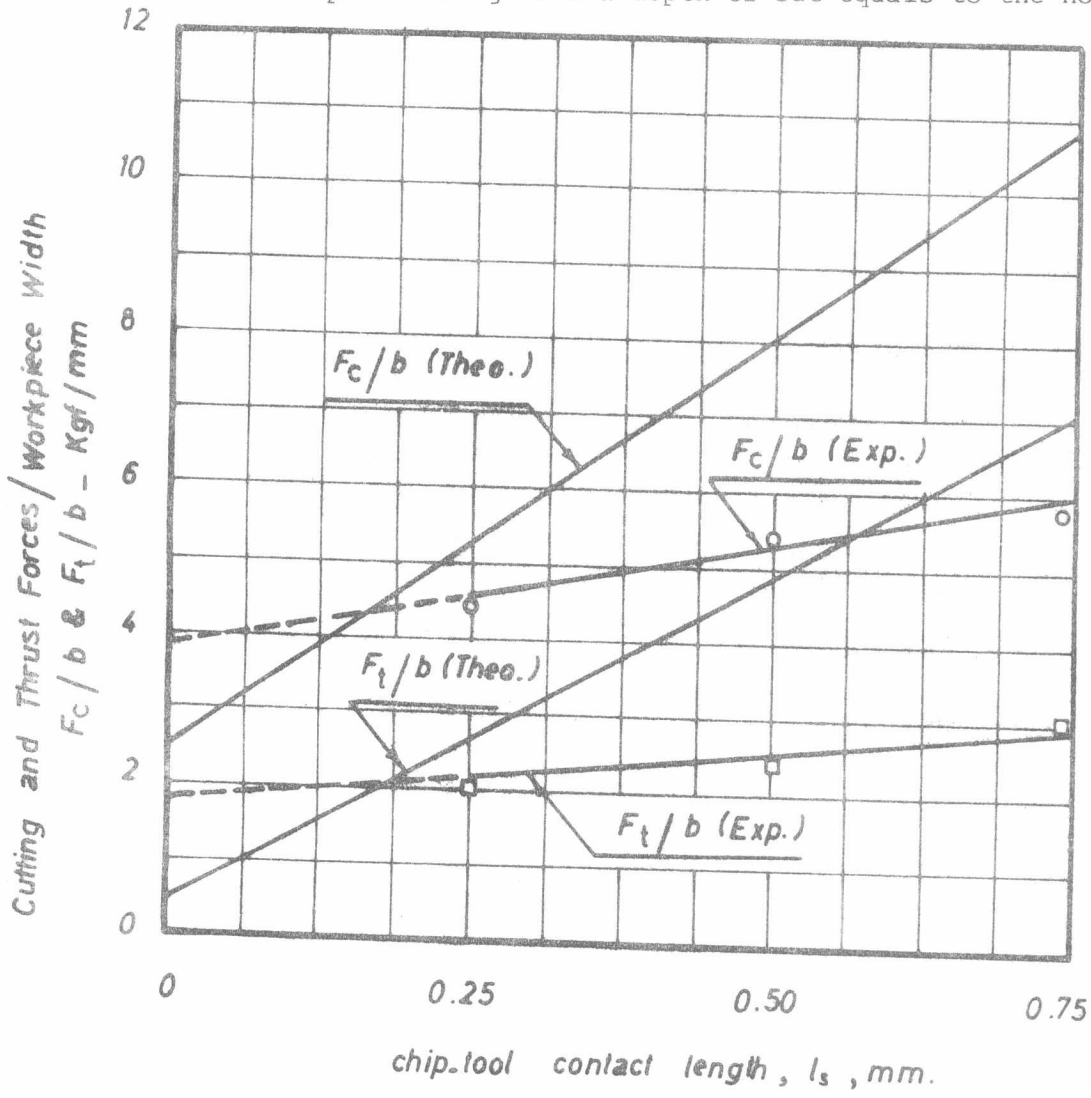

Fig.3. Relationships between force components per unit workpiece width and chip-tool contact length

height (H) being equal to $\{r(1 + \sin\alpha)\}$. Reliance is made on published data [7] by taking (r) as being equal to 0.046 mm. Material yield shear stress (τ) was computed using Merchant Force circle to be about 8 kg/mm^2. As can be seen from Fig.(3) considerable variations exist between theory and experiment. It is believed that this is due to the great approximation in applying Merchant theory for τ computation, especially for low depths of cut and small positive rake angles. It is unfortuante that neither τ nor r were determined from separate experiments. Reliance was made, therefore, on published data of the assessment of nose radius. That is of course is highly imprecise since the included tool angle is only one of several factors controlling sharp tool nose radius.

REFERENCES

1- Abdel Moneim, M.Es. and Serutton, R.F., "Tool Edge Roundness and Stable Build-up Formation in Finish Machining", Trans.A.S.M.E., Series B, J. Engg. for Industry, 96, 1258-1267, (1974).
2- AbdEl Moneim, M.Es., "Letter to the editor-Comments on Transition From Ploughing to Cutting during Machining with Blunt Tools", Wear, 63, 303-318, (1980).
3- El Khabeery, M.M., "A Study of Some Aspects of Metal Machining using Controlled Contact Length Tools", Ph.D, Thesis, North Carolina State University, U.S.A. (1982).
4- Johnson, W., "An Approximate Treatment of Metal Deformation in Rolling, Rolling Contact and Rotory Forming", Int. J. Production Research, 3, 51, (1964).
5- AbdEl Moneim, M.Es. and Scrutton, R.F., "Post Plastic Machining Recovery and the Abrasive Law", Wear, 24, 1-13, (1973).
6- Komanduri, R., "Some Aspects of Machining with Negative Rake Tools Simulating Grinding," Int.J. Machine Tool Design and Research, 11, 223-232, (1971).
7- AbdEl Moneim, M.Es., "Tool Edge Roundness in Finish Machining at High Cutting Speeds", Wear, 58, 173-192, (1980).
8- Thomsen, E.G., "Application of the Mechanics of Plastic Deformation to Metal Cutting", Annals of the C.I.R.P., 14, 113, (1966).
9- Battacharyya, A. ,"On the Friction Process in Metal Cutting", Proc. 6 th Int, Machine Tool Design and Research Conf., 491 , (1965).
10- Chandresikaran, H. and Kapoor, D.V., "Photo-Elastic Analysis of Tool Chip-Interface Stresses", Trans. A.S.M.E., Series B.,J. Engg. for Industry, 87, 495, (1965).

APPENDIX

Using the Hencky equations, and assuming a constant value for τ in accordance with the suggestion of Thomsen [8], the pressure, P, acting on the tool face at this speed (120 m/min) in the absence of a sizable active build-up, may be estimated as follows;

$$P + 2\tau\Phi_m = \text{constant along an } \alpha \text{ line} \qquad (A.1)$$

The major principle stress acting in the direction parallel to the surface is tensile and if the datum direction is chosen to be the free uncut surface, then the constant in the above Hencky equation will equal to $-\tau$. It follows that

$$P = -\tau(1 + 2\Phi_m) \qquad (A.2)$$

Now it may be seen from Fig. (A.1) that $\phi = \pi/4 - \alpha$ assuming sticking friction to prevail at the surface of the tool. Therefore;

$$P \approx \tau \mid 2.571 - 2\,\alpha_f \mid$$

The analysis presented here assumes a slip-line field which is not supported by the principle of volume constancy. Howeverm the result given by Eq. (A.2) is believed to represent a first approximation in the absence of other, more reliable, information. Battacharyya [9] and Chandreskaren and Kapoor [10] applied a similar technique to the one adopted here.

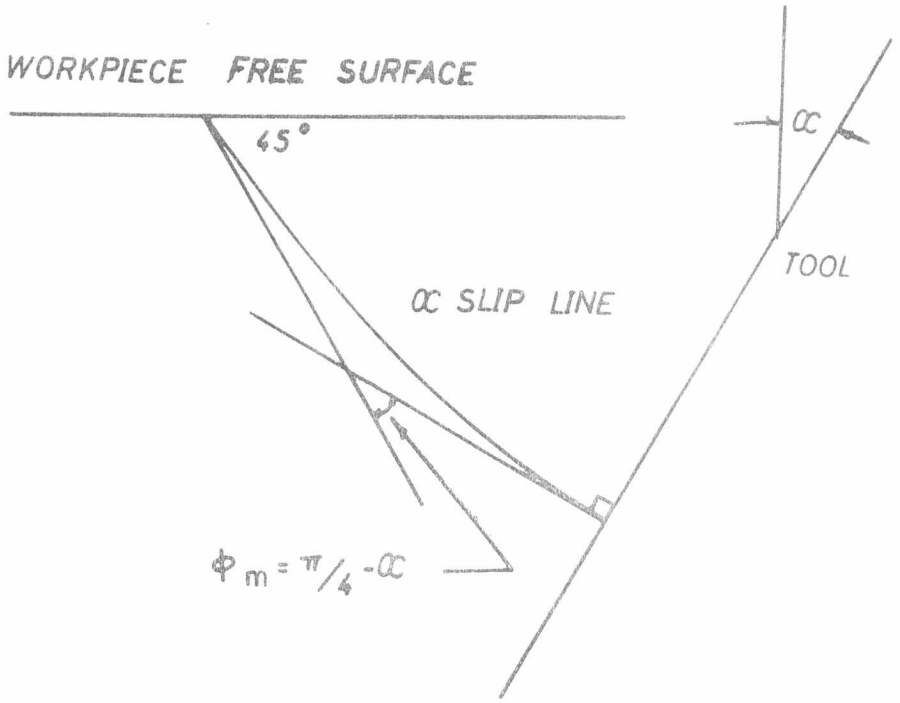

Fig.A-1 α slip line rotation between wookpiece surface and tool (sticking friction)

NOMENCLATURE

t Depth of cut.
r Sharpness radius of cutting edge.
α Tool Rake Angle.
$\alpha_f = \sin^{-1}(1 - t/r)$. The limiting value of α_f is α .
θ_o = Angle indicated in Fig. 1.
ϕ_m = Anticloc kwise rotation of ϕ - slip line indicated in Fig. A-1.
ℓ_s Chip-rake face contact length.
V_1 Nondimensional velocity indicated in hodograph show in Fig. 1.
V_{2c} Nondimensional velocity of material flow around the lower surface of the cutting tool (Fig.1).
F_e Power cutting force component per unit width normal to direction of tool motion.

F_t Thrust force component per unit width normal to direction of tool motion.

F_{er1} Power rubbing force acting over the base of the tool per unit width.

F_{er2} Power rubbing force associated with circular cylindrical velocity discontinuity beneanth tool rounded edge per unit width.

F_{er} $(= F_{er1} + F_{er2})$ Power rubbing force per unit width.

F_{ec1} Power cutting force per unit width due to chip sliding over assumed stable build-up.

F_{ec2} Power cutting force per unit width due to workpiece rubbing over lower surface of stable build-up.

F_{ec} $(= F_{ec1} + F_{ec2})$ Power cutting force per unit width.

F_e $(= F_{er} + F_{ec})$ Total power edge force per unit width, for $t \leq r(1+\sin\alpha_f)$

F_{tr} Thrust force per unit width .

F_{tc1} Thrust force per unit width due to chip action against the upper surface of the stable build-up.

F_{tc2} Thrust force per unit width due to workpiece material bearing against the lower surface of the stable build-up.

F_{tc} $(= F_{tc1} + F_{tc2})$ Thrust force per unit width due to material bearing on both surfaces of the stable build-up.

F_t $(= F_{tr} + F_{tc})$ Total thrust edge force per unit width for $t \leq r(1+\sin\alpha_f)$

Yield shear stress of the material of the workpiece during cutting.